

## Supplementary Appendix

Andrés García-García<sup>1-3</sup>, Claudia Korn<sup>1-2</sup>, María García-Fernández<sup>1-2,8</sup>, Olivia Domingues<sup>4,8</sup>, Javier Villadiego<sup>5-6,8</sup>, Daniel Martín-Perez<sup>3,8</sup>, Joan Isern<sup>3,8</sup>, José A. Bejarano-García<sup>5</sup>, Jacques Zimmer<sup>4</sup>, José A. Pérez-Simón<sup>5</sup>, Juan J. Toledo-Aral<sup>5-6,8</sup>, Tatiana Michel<sup>4,8</sup>, Matti. S. Airaksinen<sup>7,8</sup> and Simón Méndez-Ferrer<sup>1-3,\*</sup>

<sup>1</sup>*Wellcome Trust-Medical Research Council Cambridge Stem Cell Institute and Department of Hematology, University of Cambridge, Cambridge CB2 0PT, United Kingdom*

<sup>2</sup>*National Health Service Blood and Transplant, Cambridge Biomedical Campus, Cambridge CB2 0PT, United Kingdom*

<sup>3</sup>*Centro Nacional de Investigaciones Cardiovasculares (CNIC), 28029 Madrid, Spain*

<sup>4</sup>*Department of Infection and Immunity, Luxembourg Institute of Health, L-4354 Esch-sur Alzette, Luxembourg*

<sup>5</sup>*Instituto de Biomedicina de Sevilla-IBiS (Hospital Universitario Virgen del Rocío/CSIC/Universidad de Sevilla), 41013 Seville, Spain*

<sup>6</sup>*Departamento de Fisiología Médica y Biofísica, Universidad de Sevilla, 41009 Seville, Spain*

<sup>7</sup>*Neuroscience Center and Department of Anatomy, Faculty of Medicine, FI-00014 University of Helsinki, Helsinki, Finland*

<sup>8</sup>*These authors contributed equally*

\*Corresponding author:

Simón Méndez-Ferrer, PhD

E-mail: sm2116@medshcl.cam.ac.uk

Long Road, Box 96  
Cambridge CB2 0PT, UK  
Tel: +44 (0) 1223 588 070  
Fax: +44 (0) 1223 588155

## Supplementary Methods

### Cell lines

MS-5 cells, a stromal cell line established by irradiation of adherent cells in long-term bone marrow cultures and purchased from ATCC, were grown in monolayers in  $\alpha$ -MEM supplemented with 10% FBS, 2 mM L-glutamine and 2 mM sodium pyruvate (Life Technologies-Invitrogen, Carlsbad, USA). Cells were treated with acetylcholine (ach; 10  $\mu$ M, Sigma) or PBS for 6h. All cultures were maintained with 1% penicillin–streptomycin (Invitrogen) at 37 °C in a water-jacketed incubator with 5% CO<sub>2</sub> and 1:5 split with 0.05% trypsin-EDTA (Invitrogen) every three or four days, when cells reached about 80% confluence. Routine tests confirmed the absence of mycoplasma contamination in the cultures.

### BM, spleen and fetal liver cell extraction, flow cytometry and fluorescence-activated cell sorting

For BM hematopoietic cell isolation, bones were crushed in a mortar and filtered through a 40- $\mu$ m strainer to obtain single cell suspensions. Samples were depleted of red blood cells by lysis in 0.15 M NH<sub>4</sub>Cl for 10 min at 4°C. Blood samples were directly lysed.

Cells were incubated with the appropriate dilution (2-5  $\mu$ g/ml) of fluorescent antibody conjugates and 4',6-diamidino-2-phenylindole (DAPI) for dead cell exclusion, and analyzed on LSRFortessa flow cytometer (BD Biosciences, Franklin Lakes, NJ) equipped with FACSDiva Software (BD Biosciences). The following antibodies were used: fluorescent CD45.2 (104), B220 (RA3-6B2), CD11b (M1/70), CD3 $\epsilon$  (145-2C11), Ly-6G (1A8), CD90 (53-2.1), sca-1 (E13-161.7), CD106 (429; MVCAM.A) and biotinylated lineage (lin) antibodies (CD11b, Gr-1, Ter119, B220, CD3 $\epsilon$ ) (BD Biosciences); c-kit (2B8) and Cxcr4 (2B11) (Life Technologies-eBioscience); CD150 (TC15-12F12.2), CD41 (MWRReg30) and Sca-1 (D7) (BioLegend). Biotinylated antibodies were detected with fluorochrome-conjugated streptavidin (BD Biosciences).

To analyze nestin<sup>+</sup> cells, bones were cleaned off surrounding tissue, crushed in a mortar with a pestle, and digested with collagenase (catalogue number C2674, Life Technologies-Sigma; 0.25% collagenase in PBS supplemented with 20% fetal bovine serum) in water bath at 37°C for 30 min with agitation. Cells were filtered through a 40- $\mu$ m strainer and erythrocytes were lysed as described above. The resulting BM-enriched cell suspensions were pelleted, washed and resuspended in PBS containing 2% FCS for further analyses. BM stromal CD45<sup>-</sup> (30-F11) CD31<sup>-</sup> (MEC 13.3) Ter119<sup>-</sup> cells were further

purified according to GFP fluorescence using a LSRFortessa flow cytometer (BD Biosciences) for immunophenotypic analysis.

To separate endosteal and non-endosteal nestin<sup>+</sup> cells, we gently flushed the long bones and digested both the flushed fraction and the remaining bone samples with collagenase (catalogue number C2674, Sigma; 0.25% collagenase in PBS supplemented with 20% fetal bovine serum) in a water bath at 37°C for 30 min with agitation.

### **Long-term competitive repopulation assay**

To measure circulating HSCs, various blood volumes (75, 150 and 300 µl) obtained from (CD45.2) 8-week-old male *Gfra2*<sup>-/-</sup> mice and control *Gfra2*<sup>+/-</sup> littermates were mixed with  $2 \times 10^5$  BM nucleated cells from CD45.1 C57BL/6 mice in 200 µl sterile PBS and i.v. transplanted into the lethally-irradiated CD45.1 C57BL/6 mice. At various time points after transplantation (4, 8, 12 and 16 weeks), peripheral blood nucleated cells were collected from recipients. Cells were stained with fluorescent-conjugated antibodies against B220, Mac1 and CD90 antigens, and analyzed by fluorescence-activated cell sorting. The HSC concentrations were calculated using ELDA software.<sup>59</sup>

### **Homing of hematopoietic progenitors**

To study BM HSPC homing in conditioned recipients, *Gfra2*<sup>-/-</sup> mice and control *Gfra2*<sup>+/-</sup> mice were lethally irradiated (<sup>137</sup>Cs source, 12 Gy whole body irradiation, split in two doses 6+6). After 3h,  $5 \times 10^6$  nucleated cells from *Gfra2*<sup>-/-</sup> mice or control *Gfra2*<sup>+/-</sup> mice were injected (i.v.) in 200 µl PBS into each recipient mouse. To study BM HSPC homing in unconditioned recipients, we enriched donor cells in HSPCs by incubating BM nucleated cells obtained from CD45.1 C57BL/6 or *Gfra2*<sup>-/-</sup> mice with biotinylated lineage antibodies as above, followed by addition of streptavidin beads (BD Bioscience) and magnetic depletion.  $5 \times 10^6$  hematopoietic lineage-depleted CD45.1<sup>+</sup> WT or *Gfra2*<sup>-/-</sup> nucleated cells were intravenously injected in 200 µl PBS into *Gfra2*<sup>-/-</sup>, control *Gfra2*<sup>+/-</sup> (both CD45.2) or CD45.1<sup>+</sup> WT mice. HSPC homing was assessed at different ZT after transplantation. BM and the blood were harvested and used for colony-forming units in culture (CFU-C) assay as described below, and for flow cytometry analysis.

### **Colony-forming units in culture (CFU-C) assay**

For CFU-C assay from blood samples, diluted-blood samples were layered carefully over 2 ml of Lympholyte-M (Cedarlane, Burlington, Canada). Tubes were centrifuged at RT for 25 min, 1350 rpm with slow acceleration and without rotor brake. Blood nucleated cells were seeded in each well in CFU-C medium, as previously described.<sup>32</sup> Colonies were scored after 7 days in culture.

### ***In vivo* treatments**

We used the following antibodies for pharmacological homing blockade experiments. Rat monoclonal antibodies against P-selectin (clone RB40.34) and mouse  $\alpha_4$  integrin (clone PS/2) were purified from hybridoma supernatants and subjected to potential endotoxin decontamination with a polymyxin B column (Detoxi-Gel; Life Technologies-Pierce Biotechnology Inc.). Rat anti-mouse E-selectin Ab (clone 9A9) was a gift from B. Wolitzky. Control rat IgG was obtained from Sigma. Mice were injected with 1 mg/kg antibody (i.v.).

For pharmacological parasympathetic blockade experiments, mice were i.p injected with mecamlamine (3mg/kg), hexamethonium (20mg/kg), scopolamine (3mg/kg), methylatropine nitrate (3mg/kg) or vehicle at ZT5. Mice were culled and analyzed at indicated ZTs.

For pharmacological sympathetic blockade experiments, mice were i.p injected with selective antagonists of the  $\beta_2$ -adrenergic receptor (ICI 118.551), the  $\beta_3$ -adrenergic receptor (SR59230A) (Sigma, 5 mg/kg in 0.9% NaCl) or vehicle solution. Mice were culled and analyzed at indicated ZTs.

### **Immunofluorescence**

Immunofluorescence staining of skulls previously fixed in 2% PFA for 2h was performed as follows. Tissues were permeabilised and blocked with 0.5% Triton X-100 (Sigma) in TNB buffer (0.1 M Tris-HCl, pH 7.5, 0.15 M NaCl, 0.5% blocking reagent (PerkinElmer, Waltham, MA, USA) overnight at 4°C. Endogenous peroxidase was blocked incubating with 0.4% H<sub>2</sub>O<sub>2</sub>/PBS for 2h. After washing, endogenous biotin was blocked with Avidin/Biotin blocking kit (VectorLabs, Burlingame, CA, USA). Primary antibodies diluted in 0.1% Triton X-100/TNB were incubated for 2-3 days at 4°C. Repetitive washes were performed with 0.1% Triton X-100 in PBS for 8h and secondary antibodies diluted in TNB were incubated overnight at 4°C. Repetitive washes were performed with 0.1% Triton X-100 in PBS for 4h. Tyrosine hydroxylase staining included an amplification step using the Vectastain Elite ABC Kit (Vector Labs) and Cy3-Tyramide (PerkinElmer). Stained skulls were counterstained for 5 min with 5  $\mu$ M

DAPI and rinsed with PBS. We used the following primary antibodies: tyrosine hydroxylase (1:1000, rabbit polyclonal antibody, Millipore), Gfra2 (1:200, goat polyclonal antibody, R&D), VACht (1:100, goat polyclonal Merck) and CD31 (1:200, rat polyclonal antibody, BD Biosciences). Confocal mouse images were acquired with a laser scanning confocal microscope (Zeiss, Oberkochen, Germany, LSM 700). For all stainings, control and experimental samples were processed simultaneously and at least 3 different sections per animal were blindly analyzed using ImageJ software.

## **ELISA**

Cxcl12 protein levels were measured by conventional ELISA. Briefly, 96-well plates were coated overnight at 4°C with 2 µg/ml of monoclonal CXCL12/SDF-1 antibody (MAB350, R&D Systems, Las Vegas, NE, USA). After blocking, BM extracellular fluids were incubated with the antibody for 2h at room temperature, followed by addition of biotinylated anti-human and mouse CXCL12/SDF-1 antibody (BAF310, R&D). Streptavidin-horseradish peroxidase conjugate (RPN1231V, Dako-Agilent Technologies, Santa Clara, CA, USA) was used to detect the signal, and the reaction was developed with horseradish peroxidase substrate (TMB, ES001-500ML, Chemicon, MERCK Millipore, Darmstadt, Germany). Standard curve was performed with recombinant SDF-1 alpha (350-NS, R&D).

ELISA for norepinephrine/epinephrine (Bi-CAT ELISA Alpco Diagnostics, Salem, NH, USA) was performed according to the manufacturers' recommendations.

Acetylcholinesterase measures were performed with Acetylcholinesterase Activity Assay Kit (Sigma).

## **RNA isolation, reverse transcription and quantitative real-time PCR (Q-PCR)**

Total RNA extraction was performed with TRIzol (Life Technologies), followed by treatment with DNase to eliminate contaminating genomic DNA with RNase-free DNase Set (Qiagen, Hilden, Germany) and RNA clean-up with RNeasy mini kit (Qiagen). RNA concentration was measured using Nanodrop (Life Technologies-ThermoScientific). Reverse transcription was performed using the Reverse Transcription System (Promega, Madison, USA), following the manufacturer's recommendations. mRNA expression was measured by quantitative real-time RT-PCR using the classical SYBR green method. Specific oligonucleotides pairs were mixed with SYBR Green PCR Master Mix (Applied Biosystems) and reactions were run in an ABI PRISM 7900HT Sequence Detection System (Applied Biosystems). Analysis was performed using SDS software (Applied Biosystems). The expression level of each gene

was determined by the relative standard curve method, using a standard curve prepared from serial dilutions of a mouse or human reference total RNA (Clontech-Takara Bio, Shiga, Japan). The expression level of each gene was calculated by interpolation from the standard curve. All values were normalized to *Gapdh* as the endogenous control. The sequence of oligonucleotides used for quantitative real-time RT-PCR are shown:

Gene	Forward	Reverse
<i>Cxcl12</i>	CGCCAAGGTCGTCGCCG	TTGGCTCTGGCGATGTGGC
<i>Kitl</i>	CCCTGAAGACTCGGGCCTA	CAATTACAAGCGAAATGAGAGCC
<i>Gfra2</i>	TTTAACATGATCTTGGCAAACG	AGCGGAGGGTTTCGTCTAA
<i>Nrtn</i>	TGAGGACGAGGTGTCCTTCCT	AGCTCTTGCAGCGTGTGGTA
<i>Adrb2</i>	AAGAATAAGCCCGAGTGGT	GTAGGCCTGGTTCGTGAAGA
<i>Adrb3</i>	AAACTGGTTGCGAACTGTGG	TAACGCAAAGGGTTGGTGAC
<i>Vcam1</i>	GACCTGTTCCAGCGAGGGTCT	CTTCCATCCTCATAGCAATTAAGGTG
<i>Sele</i>	TGAAGTGAAGGGATCAAGAAGACT	GCCGAGGGACATCATCACAT
<i>Selp</i>	TCCAGGAAGCTCTGACGTACTTG	GCAGCGTTAGTGAAGACTCCGTAT
<i>Gapdh</i>	TGTGTCCGTCGTGGATCTGA	CCTGCTTCACCACCTTCTTGA

### Quantification and statistical analysis

We used similar response variables for the calculation of sample size. For each hypothesis, the total cell number and composition of the different cell populations was determined by flow cytometry, in peripheral blood (after each treatment) and in the bone marrow (at the end of the experiment). The compared groups were set similarly in all procedures. For each scenario, we established the number of conditions in which to test the hypothesis, and two groups were randomly assigned to each condition (control group and experimental group). Results were scored blindly. Data shown in figures are means  $\pm$  SEM; n and p values are indicated in each chart bar or figure. One Way ANOVA and Bonferroni comparison were used for multiple group comparisons, and unpaired two-tailed t tests for two-group comparisons. The data met the assumptions of the tests. Significant statistical differences between groups were indicated as: \*  $p < 0.05$ ; \*\*  $p < 0.01$ ; \*\*\*  $p < 0.001$ . When ANOVA was used, the p value of the ANOVA test is shown in the bar chart above the pairwise comparisons, whereas the p value of the pairwise comparisons is indicated with asterisks. Statistical analyses and graphics were carried out with GraphPad Prism 5 software and Microsoft Excel.

## Key resources Table

REAGENT or RESOURCE	SOURCE	IDENTIFIER
Antibodies		
PE-Cy <sup>TM</sup> 7 Mouse Anti-Mouse CD45.1 Clone A20	BD Biosciences	Cat#560578
APC-Cy <sup>TM</sup> 7 Mouse Anti-Mouse CD45.2 Clone 104	BD Biosciences	Cat#560694
FITC Rat Anti-Mouse CD45R/B220 Clone RA3-6B2	BD Biosciences	Cat#553088
APC Rat Anti-Mouse CD11b Clone M1/70	BD Biosciences	Cat#553312
PerCP-Cy <sup>TM</sup> 5.5 Hamster Anti-Mouse CD3e Clone 145-2C11	BD Biosciences	Cat#561108
PE Rat Anti-Mouse Ly-6G Clone 1A8	BD Biosciences	Cat#561104
PE Rat Anti-Mouse CD90.2 Clone 53-2.1	BD Biosciences	Cat#553005
PE Rat Anti-Mouse CD106 Clone 429 (MVCAM.A)	BD Biosciences	Cat#561613
PE Rat Anti-Mouse Ly-6A/E Clone E13-161.7	BD Biosciences	Cat#553336
Biotin Mouse Lineage Panel (CDBBb, Gr-1, Ter119, B220, CD3e)	BD Biosciences	Cat#559971
Anti-Mouse CD117 (c-Kit) PE-Cyanine7	eBioscience	Cat#25-1171-82
PE Rat Anti-Mouse Cxcr4 Clone 2B11	eBioscience	Cat#12-9991-82
APC anti-mouse CD150 (SLAM) Antibody Clone TC15-12F12.2	BioLegend	Cat#115910
PerCP/Cy5.5 anti-mouse CD41 antibody Clone MWRReg30	BioLegend	Cat#133918
Streptavidin APC-Cy <sup>TM</sup> 7	BD Biosciences	Cat#554063
Biotin Rat Anti-Mouse CD45 Clone 30-F11	BD Biosciences	Cat#553077
Biotin Rat Anti-Mouse CD31 Clone MEC 13.3	BD Biosciences	Cat#553371
Biotin Rat Anti-Mouse TER-119/Erythroid Cells Clone TER-119	BD Biosciences	Cat#553672
Purified monoclonal anti-mouse P-selectin Clone RB40.34	N/A	N/A
Purified monoclonal anti-mouse $\alpha$ 4 integrin Clone PS/2	N/A	N/A
Rat anti-mouse E-selectin Clone 9A9	B. Wolitzky	N/A
Human/Mouse CXCL12/SDF-1 Antibody	R&D Systems	Cat#MAB350
Human/Mouse CXCL12/SDF-1 Biotinylated Antibody	R&D Systems	Cat#BAF310
Rabbit polyclonal tyrosine hydroxylase antibody	Millipore	Cat#AB152
Goat Anti-Gfra2 antibody	R&D	Cat#AF429
Polyclonal goat anti-Vesicular Acetylcholine Transporter antibody	Merck	CAT#ABN100
Chemicals, Peptides, and Recombinant Proteins		
Collagenase from Clostridium histolyticum	Sigma-Aldrich	Cat#C2674
BD IMag <sup>TM</sup> Streptavidin Particles Plus	BD Biosciences	Cat#557812
Lympholyte <sup>®</sup> -M Cell Separation Media	Cedarlane	Cat#CL5031
Acetylcholine chloride	Sigma-Aldrich	Cat#A6625
Atropine methyl nitrate	Sigma-Aldrich	Cat#SML0732
Mecamylamine hydrochloride	Sigma-Aldrich	Cat#M9020
Scopolamine hydrobromide	Sigma-Aldrich	Cat#PHR1470
Hexamethonium bromide	Sigma-Aldrich	Cat#H0879
ICI118,551 hydrochloride	Sigma-Aldrich	Cat#I127
SR 59230A	Sigma-Aldrich	Cat#S8688
Detoxi-Gel <sup>TM</sup> Endotoxin Removing Columns	Pierce Biotechnology Inc	N/A

Peroxidase-Conjugated Streptavidin	DAKO	Cat#P0397
TMB/E Single Reagent, Blue color, Horseradish Peroxidase Substrate	Millipore	Cat#ES001
Recombinant Human/Rhesus Macaque/Feline CXCL12/SDF-1 alpha	R&D Systems	Cat#350-NS
Critical Commercial Assays		
TSA Cyanine 3 Tyramide Reagent Pack	PerkinElmer	Cat#SAT704A001E A
VECTASTAIN® Elite® ABC-HRP Kit	VectorLabs	Cat#PK6100
Bi-CAT (Epinephrine & Norepinephrine) ELISA	ALPCO	Cat#17-BCTHU-EO2.1
Acetylcholinesterase Activity Assay Kit	Sigma-Aldrich	Cat#MAK119
Experimental Models: Cell Lines		
MS-5 murine stromal cell line	N/A	N/A
Experimental Models: Organisms/Strains		
Mouse: <i>Gfra2</i> <sup>-/-</sup>	REF 19	N/A
Mouse: <i>Nes-gfp</i>	G. Enikolopov; REF 20	N/A
Mouse: <i>Adrb2tm1Bkk/J</i>	G. Karsenty; REF 21	N/A
Mouse: FVB/N- <i>Adrb3</i> <sup>tm1Lowl</sup>	The Jackson Laboratory	JAX: 006402
Mouse: <i>B6;129X1-Nrtn</i> <sup>tm1Jmi/J</sup> ( <i>Nrtn</i> <sup>-/-</sup> )	The Jackson Laboratory	JAX: 012238
Mouse: <i>B6.SJL-Ptprca Pepcb/BoyJ</i>	The Jackson Laboratory	JAX: 002014
Mouse: <i>C57BL/6J</i>	The Jackson Laboratory	JAX: 000664
Sequence-Based Reagents		
Primers for quantitative real-time RT-PCR, see STAR Methods		
RNeasy Mini Kit	QIAGEN	Cat#74104
Reverse Transcription System	Promega	Cat#A3500
Software and Algorithms		
FACSDiva Software	BD Biosciences	
ELDA software	REF 59	
ImageJ Software	Java	
GraphPad Prism	GraphPad	
Microsoft Excel	Microsoft Office	



**Table S1**

Features	<i>Gfra2</i> <sup>-/-</sup> mouse	<i>Nrtn</i> <sup>-/-</sup> mouse
Central parasympathetic activity	Decreased <sup>19</sup>	Unaltered <sup>22</sup>
Sympathetic noradrenergic activity	Increased	Unaltered
BM HSPC and leukocytes maintenance	Decreased	Unaltered
HSPC and leukocytes egress (via $\beta_3$ -AR)	Increased	Unaltered
BM local sympathetic cholinergic activity	Decreased <sup>23</sup>	Increased
Cell adhesion molecules (via $\beta_2$ -AR and Chrn)	Increased	Decreased

**Table S1. Comparative features affecting migration of HSPCs and leukocytes in mice lacking central parasympathetic activity and peripheral sympathetic cholinergic innervation (*Gfra2*<sup>-/-</sup>), or with preserved central parasympathetic activity and increased peripheral sympathetic cholinergic innervation (*Nrtn*<sup>-/-</sup>).**

*Gfra2*<sup>-/-</sup> mice exhibit markedly deficient central parasympathetic activity,<sup>19</sup> which correlates with exacerbated sympathetic noradrenergic activity. At night, increased epinephrine concentration in blood predominantly signals through  $\beta_2$ -AR to increase vascular cell adhesion and BM homing. At daytime, local sympathetic noradrenergic activity signals through  $\beta_3$ -AR to reduce Cxcl12 expression and trigger BM egress, which causes accumulation of circulating HSPCs and WBCs.

In sharp contrast, *Nrtn*<sup>-/-</sup> mice exhibit increased sympathetic cholinergic innervation, which locally reduces vascular cell adhesion. However, unlike in *Gfra2*<sup>-/-</sup> mice, central parasympathetic activity is not severely compromised in *Nrtn*<sup>-/-</sup> mice.<sup>22</sup> Consequently, *Nrtn*<sup>-/-</sup> mice do not show altered sympathetic noradrenergic activity or circadian trafficking of HSPCs and leukocytes.

Figure S1

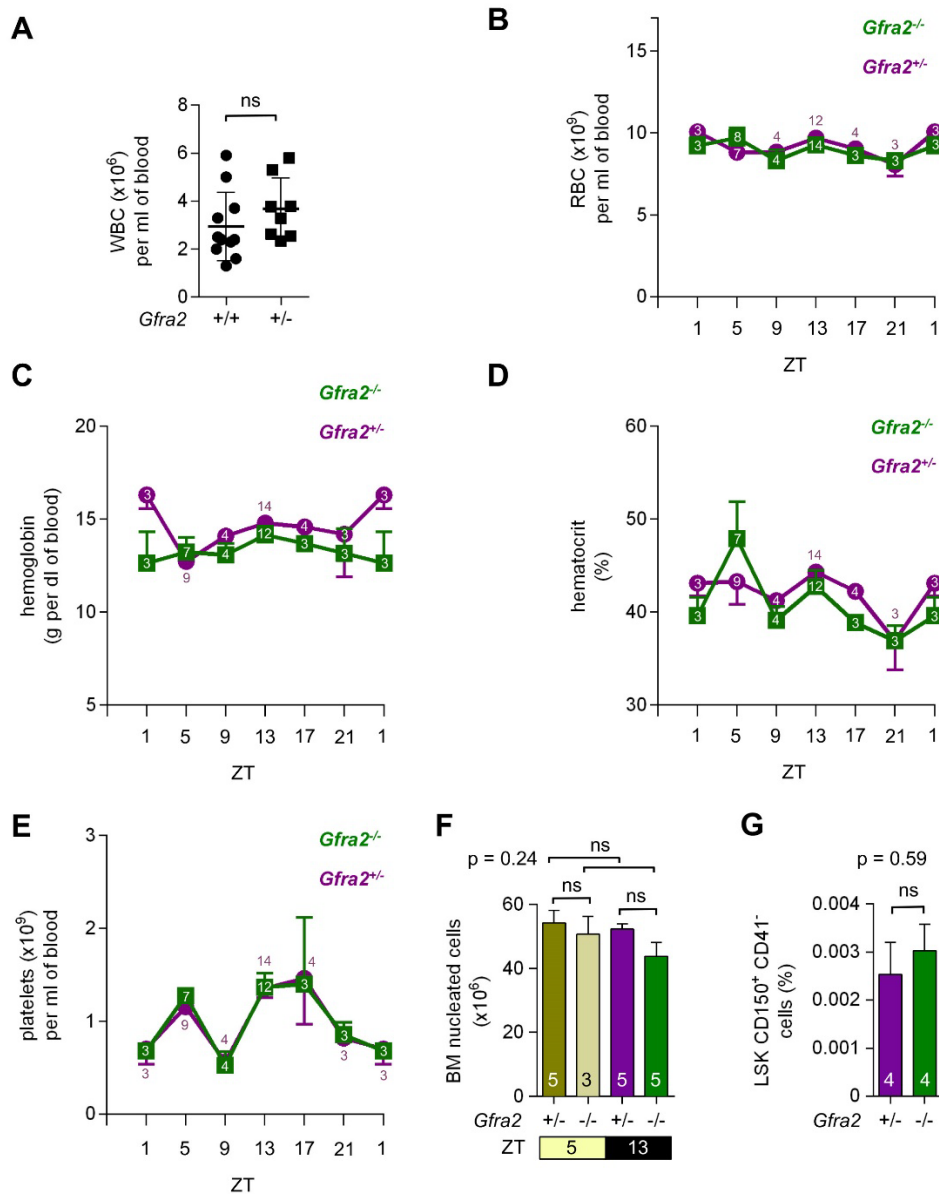


**Figure S1. Parasympathetic-deficient mice show altered circadian migration of HSPCs and leukocytes (Figure 1) but do not exhibit broad hematopoietic defects.**

(A) Concentration of circulating white blood cells (WBC) in WT *Gfra2*<sup>+/+</sup> mice and heterozygous *Gfra2*<sup>+/-</sup> mice at ZT13. Each dot represents a mouse.

(B-E) Concentration of (B) red blood cells (RBC), (C) hemoglobin, (D) hematocrit and (E) platelets at the specified ZT. ZT1 has been duplicated to facilitate viewing.

(F) BM nucleated cell number in *Gfra2*<sup>-/-</sup> and control *Gfra2*<sup>+/-</sup> mice at indicated ZT.

(G) Frequency of BM lin<sup>-</sup> sca-1<sup>+</sup> c-kit<sup>+</sup> CD150<sup>+</sup> CD41<sup>-</sup> HSCs at ZT13.

(A-G) Data are means  $\pm$  SEM; n and p values (multivariate analysis for >2 groups) are indicated. (A, G) Unpaired two-tailed *t* test. (B-E) Multiple two-tailed test. (F) One-way ANOVA and Bonferroni comparisons.

## Figure S2

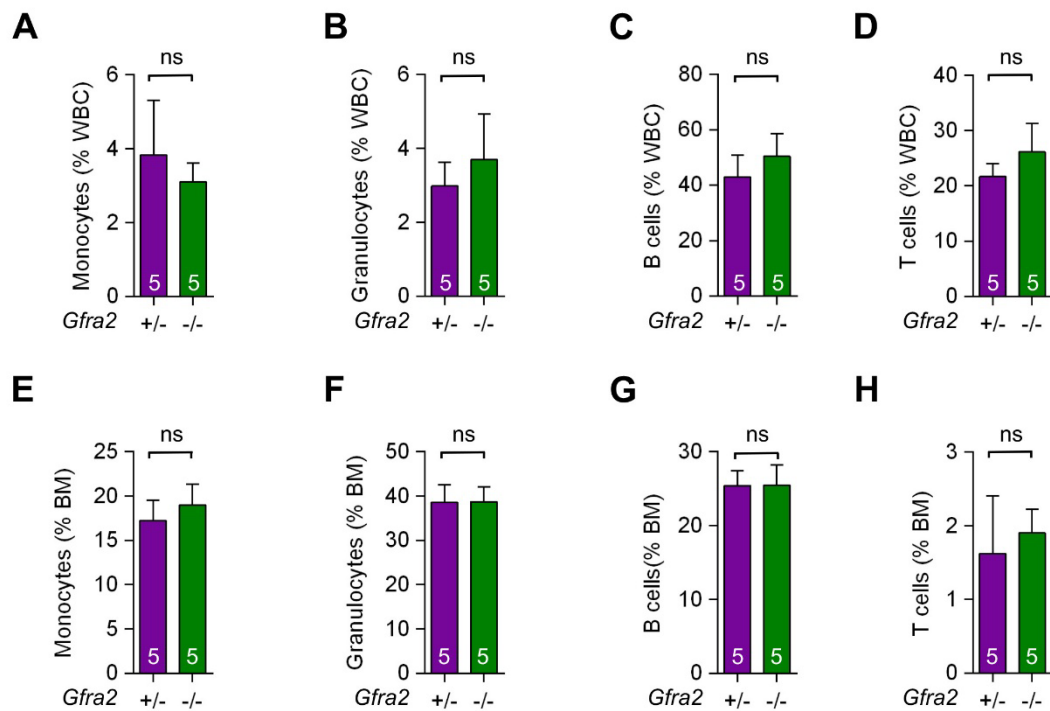


**Figure S2. Parasympathetic-deficient mice show altered circadian migration of HSPCs and leukocytes (Figure 1) but exhibit normal frequencies of mature hematopoietic cells.**

(A-D) Frequency of monocytes (A), granulocytes (B), B cells (C) and T cells (D) in the peripheral blood of *Gfra2*<sup>-/-</sup> and control *Gfra2*<sup>+/-</sup> mice at ZT13.

(E-H) Frequency of monocytes (E), granulocytes (F), B cells (G) and T cells (H) in the BM of *Gfra2*<sup>-/-</sup> and control *Gfra2*<sup>+/-</sup> mice at ZT13.

(A-H) Data are means  $\pm$  SEM; n and p values are indicated. Unpaired two-tailed *t* test.

**Figure S3. Increased BM homing in parasympathetic-deficient mice.**

(A-B) Frequencies of WT CD45.1<sup>+</sup> (A) lin<sup>-</sup> sca1<sup>-</sup> c-kit<sup>+</sup> hematopoietic progenitors and (B) lin<sup>-</sup> cells at ZT2 that homed during the night to the BM after i.v. transplantation in non-irradiated *Gfra2*<sup>-/-</sup> mice or control *Gfra2*<sup>+/-</sup> mice at ZT10.

(C) Representative flow cytometry diagrams of CD45.1<sup>+</sup>lin<sup>-</sup>sca1<sup>+</sup>c-kit<sup>+</sup> (LSK) cells detected in the BM of mice in Fig. 3D.

(A-B) Data are means  $\pm$  SEM; n and p values are indicated. Unpaired two-tailed *t* test. \*  $p < 0.05$ ; \*\*  $p < 0.01$ .

**Figure S4. The parasympathetic nervous system inhibits  $\beta_2$ -adrenergic-dependent vascular adhesion and BM homing.**

(A) Vcam1 expression (MFI; mean fluorescence intensity) in CD31<sup>+</sup> endothelial cells from *Gfra2*<sup>-/-</sup> and control *Gfra2*<sup>+/-</sup> mice.

(B) Frequencies of donor-derived WT CD45.1<sup>+</sup> lin<sup>-</sup> cells at ZT2 that homed during the night to the BM after i.v. transplantation (at ZT10) in non-irradiated *Gfra2*<sup>-/-</sup> mice or control *Gfra2*<sup>+/-</sup> mice pre-conditioned with saline or  $\beta_2$  adrenergic antagonist (ICI118,551) 4h before transplantation.

(A-B) Data are means  $\pm$  SEM; n and p values are indicated. One-way ANOVA and Bonferroni comparisons. \* p < 0.05.

**Figure S5. *Gfra2*<sup>-/-</sup> mice exhibit normal Cxcr4 expression in WBCs.**

(A) Cxcr4 expression (MFI; mean fluorescence intensity) in WBCs from *Gfra2*<sup>-/-</sup> and WT mice at ZT13. Data are means  $\pm$  SEM; n and p values are indicated. Unpaired two-tailed *t* test.

(B) Representative flow cytometry histogram showing Cxcr4 expression.

## Figure S6

**Figure S6. Local cholinergic signals modulate  $\beta_3$ -AR (Figure 6) but not  $\beta_2$ -AR BM expression.**

(A) *Adrb2* mRNA expression in MS-5 cell line cultures treated with vehicle or acetylcholine (10  $\mu$ M) for 6h.

(B) *Adrb2* mRNA expression in the BM of WT mice treated with acetylcholine antagonists (i.p) at ZT5.

(A-B) Data are means  $\pm$  SEM; n and p values are indicated. Unpaired two-tailed *t* test.

## Figure S7

**Figure S7. BM sympathetic noradrenergic innervation and Cxcl12 expression are not affected in *Nrtn*<sup>-/-</sup> mice.**

(A-B) Representative immunofluorescence of TH<sup>+</sup> sympathetic noradrenergic nerve fibers (red) in the skull of WT and *Nrtn*<sup>-/-</sup> mice. Scale, 100  $\mu$ m.

(C) Quantification of TH<sup>+</sup> sympathetic noradrenergic nerve fibers from the skull of *Nrtn*<sup>-/-</sup> and WT mice.

(D) Cxcl12 concentration in BM extracellular fluid (BMECF) of *Nrtn*<sup>-/-</sup> and WT mice at ZT13.

(C-D) Data are means  $\pm$  SEM; n and p values are indicated. Unpaired two-tailed *t* test.